# OPTIMIZATION OF PERFORMANCE OF BAMBOO MAT CORRUGATED SHEETS USING RESPONSE SURFACE METHODOLOGY

*Li Gao*

Associate Professor
E-mail: gaoli@caf.ac.cn

*Shupin Luo**

Assistant Professor
E-mail: luosp@caf.ac.cn

*Wenjing Guo*

Professor
Research Institute of Wood Industry
Chinese Academy of Forestry
No 1 Dongxiaofu, Haidian District
Beijing 100091, China
E-mail: guowj@caf.ac.cn

(Received November 2018)

**Abstract.** In this study, a bamboo composite with a corrugated structure, bamboo mat corrugated sheets (BMCS), was manufactured. As subset of the response surface methodology, Box–Behnken design was used for designing experiments, statistically modeling the processing conditions–properties relationships, and for identification of the potentially optimum conditions for BMCS. Three variables (MC, pressing temperature, and pressing time) at three levels were studied. Results showed that all the tested properties (deformation ratio, failing load, bending strength, and impact strength) were best described by quadratic regression models. Keeping MC at higher level significantly decreased the deformation ratio. All the three factors and interactions between any two of them were significant model terms for failing load. Pressing temperature, pressing time, and their interactions were significant model terms for bending strength. The interaction effect of MC and the other two factors was significant for impact strength. The best optimized conditions were determined using a desirability function approach to be MC 12.3%, pressing temperature 146.2°C, and pressing time 12.8 min that optimized 1.8% for deformation ratio, 542 N for failing load, 185.7 MPa for bending strength, and 36.5 kJ/$m^2$ for impact strength of BMCS.

***Keywords:*** Bamboo, corrugated structure, mechanical properties, modeling, optimization, response surface methodology (RSM).

## INTRODUCTION

Corrugated structure has long been valued as a good engineering design that can be used in a variety of applications, eg packaging, civil, marine, and mechanical engineering structures (Dayyani et al 2015; Park et al 2016). The advantages of a corrugation structure design include anisotropic nature, high capacity of energy absorption, and high stiffness-to-weight ratio (Chen et al 2013a). As a special and important nonwood forest resource, bamboo possesses advantages, including fast growth rate, high specific strength and stiffness, low cost, and low energy consumption in processing (Jiang et al 2013). In recent years, some studies have been reported developing bamboo-based composites with a corrugated structure, such as bamboo bundle corrugated laminated composites (Chen et al 2013a; Jiang et al 2013), corrugated bamboo particleboard (Yang et al 2014), and corrugated bamboo roofing sheets.

The performance of these corrugated composites depends heavily on manufacturing condition variables, such as MC, resin content, pressing

* Corresponding author


https://doi.org/10.22382/wfs-2019-xxx

temperature, and pressing time (Carlborn and Matuana 2006). Yang et al (2014) fabricated corrugated bamboo particleboards (CBP) from bamboo waste. The results showed that the static bending strength of CBP laminated with medium-density fiberboard initially increases and then decreases with increased pressing temperature from 150 to 200°C. Increasing the magnitude of the pressing temperature has a slightly positive effect on the dimensional stability properties. Chen et al (2013a) fabricated bamboo bundle laminated composite with a corrugated structure. They found that the dimensional stability of the composite was significantly different among the three directions of the composites, and it was affected by the stacking sequence of the bamboo bundles.

Bamboo mat board consists of woven mats of split bamboo pressed firmly together to form a product that resembles plywood. By soaking the mats in resin and then pressing them between two corrugated pressing plates, the corrugations are formed, denoted as bamboo mat corrugated sheets (BMCS). The sheets are durable and resistant to pest attack, severe weathering, and fire. They have very high strength-to-weight ratio, and hence, these sheets have great potential to be used in roofing, wall panels, packaging, and transportation containers (Bansal and Zoolagud 2002). Presently, limited published experimental data are available on manufacturing of BMCS, not to mention the impact of processing parameters on their properties. To achieve high performance and commercial success for products, the optimization of the fabricating process is the first key factor to be considered. Work is still needed to determine the relationships between the properties of the BMCS and the manufacturing variables. When multiple variables are involved, applying the common "one-factor-at-a-time" is costly in sense of time and reagents. Moreover, this approach does not identify the interactions between factors.

Response surface methodology (RSM) is a collection of mathematical and statistical techniques that are used for modeling and analysis of systems in which a response or output variable of interest is influenced by several input variables and the aim is to optimize this response (Nakhaei et al 2017). RSM is well applied in the characterization and optimization of processes (Carlborn and Matuana 2006). The process of developing a RSM model involves three main steps: collect the experimental data of the response, construct a model and validate its accuracy, and finally optimize the parameters to satisfy the defined desirable response variables (Yaghoobi and Fereidoon 2018a). 3D surfaces generated by RSM can help visualizing the effect of parameters on response in the entire range specified (Yaghoobi and Fereidoon 2018b). The desirability criterion available in RSM will easily help users to determine the optimum condition. To improve the performance of BMCS, a standard RSM called Box–Behnken design (BBD) was used in this work to analyze the effects of processing variables and optimize them. The advantage of BBD is that it requires only three levels for each factor, avoids experiments performed under extreme conditions, and does not involve combinations for which all factors are simultaneously at their highest or lowest points. BBD is more efficient and easier to arrange and interpret in comparison with full factorial or central composite designs.

RSM has been applied on plywood, particleboard, fiberboard, wood–rubber composite panel, and natural fiber/plastic composite. Chen et al (2013b) optimized the preparation conditions of soy flour adhesive for plywood, whereas Yu et al (2015) optimized the mechanical properties of plywood made of bamboo and discussed the effects of different process parameters on the mechanical properties of bamboo plywood. Islam et al (2012) performed BBD with desirability functions to attain the optimal flake thickness, chip MC, and press temperature that affect bending properties of particleboard. Kumar et al (2016) optimized processing parameters of medium-density fiberboard that used multiwalled carbon nanotubes reinforced urea formaldehyde resin. Zhao et al (2008) optimized the processing variables in wood–rubber composite panels with a combination binder system. Toupe et al (2014) performed a simultaneous optimization of selected factors on phase compatibilization of a flax fiber/recycled plastic composite. The optimization was performed to identify the composite composition leading to both mechanical and economic optimum. Yaghoobi and Fereidoon (2018a, 2018b, 2018c) applied BBD for modeling and optimizing the effects of fiber load, fiber length, and compatibilizer content on impact strength, tensile, and flexural properties of polypropylene/kenaf fiber/polypropylene-grafted maleic anhydride biocomposites. As far as known to the authors, no previous literature has reported on optimization of the manufacturing of BMCS using the RSM approach.

In this present study, the effects of MC, pressing temperature, and pressing time on the properties of BMCS were evaluated using a BBD to statistically model the system. Responses including deformation ratio, failing load, bending strength, and impact strength were determined for assessing the quality of sheets. The processing parameters will be optimized for achieving high-quality sheets through numerical parameter optimization.

## MATERIALS AND METHODS

### Materials

Moso bamboo (*Phyllostachys pubescens*) mat woven using tangentially oriented strips was obtained from Heqichang Bamboo Industry Corporation, Yongan, Fujian Province, China. The air-dried bamboo mat (1.0-1.2 mm thickness, 7% MC) was cut into 450 mm × 500 mm sections for subsequent use. A commercial phenol formaldehyde (PF) resin of 46% solid content and viscosity of 30 mPa·s at 23°C was obtained from the Taier Corporation, Beijing, China.

### Multivariate Experimental Design

The experiments were designed based on BBD of RSM using Design-Expert software v8.0. Three variables (MC, pressing temperature, and pressing time) and their actual experimental range and coded levels (−1, 0, and +1 for low, middle, and high values, respectively) are given in Table 1. The applied BBD yielded a total of 17 runs in a random order, including five central points ($N = 2k[k-1] + C_0 = 17$ runs, where $N$ is the total number of experiments required, $k$ and $C_0$ is the number of factors and the central points) (Yaghoobi and Fereidoon 2018b). The experimental design conducted in this study is tabulated in Table 2.

A second-order polynomial model used for fitting the response to the independent variables is shown as follows (Islam et al 2012):

$$y = \beta_0 + \sum \beta_i x_i + \sum \beta_{ii} x_i^2 + \sum \beta_{ij} x_i x_j, \quad (1)$$

where $y$ is the response (properties), $\beta_0$ the intercept, and $\beta_i$, $\beta_{ii}$, $\beta_{ij}$ are the coefficients of parameters for linear, squared, and interaction effects, respectively. The evaluation of the statistical significance of the model by the $p$ values less than 0.05 was analyzed using analysis of variance (ANOVA). Five central points are used for calculating the pure error. The model regression ($R^2$), adjusted $R^2$, predicted $R^2$, and lack of fit from ANOVA were used in the determination of the quality of developed model.

### Preparation of BMCS

The PF resin was diluted to a solid content of 30%. The bamboo mat was immersed in the PF resin to obtain an impregnation amount of about 10% by adjusting immersion time, and then dried to different MC of 9%, 12%, or 15%. A QD056 hot press (Shanghai Wood-based Panel Machinery Co. Ltd., Shanghai, China) equipped with

Table 1. Actual and coded experimental variables and corresponding levels in Box–Behnken experimental design.

| Variables | Code | Level | | |
|---|---|---|---|---|
| | | Low (−1) | Middle (0) | High (+1) |
| MC (%) | *A* | 9 | 12 | 15 |
| Pressing temperature (°C) | *B* | 130 | 145 | 160 |
| Pressing time (min) | *C* | 6 | 12 | 18 |

Table 2. Box–Behnken design matrix and experimental results.

| Run no. | Coded level *A* | *B* | *C* | Deformation ratio (%) | Failing load (N) | Bending strength (MPa) | Impact strength (kJ/m$^2$) |
|---|---|---|---|---|---|---|---|
| 1 | 1 | −1 | 0 | 1.3 | 156 | 147 | 27.5 |
| 2 | 0 | 0 | 0 | 1.6 | 524 | 188.6 | 37.1 |
| 3 | 0 | 1 | 1 | 2.7 | 324 | 175 | 26.9 |
| 4 | 0 | −1 | 1 | 1.5 | 398 | 160 | 29.0 |
| 5 | −1 | −1 | 0 | 5.7 | 426 | 127.2 | 37.0 |
| 6 | 1 | 1 | 0 | 0.2 | 360 | 140.1 | 32.2 |
| 7 | 0 | 0 | 0 | 1.7 | 572 | 182.6 | 36.3 |
| 8 | 1 | 0 | 1 | 0.9 | 339 | 170.5 | 24.3 |
| 9 | 0 | 0 | 0 | 0.2 | 516 | 178.1 | 37.3 |
| 10 | 0 | −1 | −1 | 4 | 193 | 134.6 | 31.5 |
| 11 | 0 | 0 | 0 | 1.1 | 554 | 185.6 | 37.7 |
| 12 | −1 | 1 | 0 | 7.2 | 362 | 168.4 | 29.8 |
| 13 | −1 | 0 | 1 | 6.8 | 403 | 159.3 | 32.2 |
| 14 | −1 | 0 | −1 | 6.5 | 412 | 132.4 | 30.3 |
| 15 | 0 | 1 | −1 | 3.9 | 395 | 152.9 | 26.0 |
| 16 | 0 | 0 | 0 | 2.7 | 564 | 184.2 | 36.6 |
| 17 | 1 | 0 | −1 | 1.3 | 228 | 137.5 | 30.4 |

a custom-designed corrugated mold (Fig 1) was used to press the resinated mat at 5-MPa pressure and three temperature levels (130, 145, or 160°C) for different times (6, 12, or 18 min, respectively). For each BMCS, seven layers of bamboo mats were used, and they were aligned in the direction of the corrugated waves. The target density was 0.9 g/cm$^3$. Thickness gauges (6 mm thickness) were used to produce sheets at a given thickness. The corrugated sheet was produced in three replicates for each run.

## Property Testing

Before testing, all samples were conditioned in a climate chamber at 20°C and 65% RH, until constant mass was reached. Deformation ratio (ε) was determined using the following equation:

$$\varepsilon = \left( \left| \frac{d_1 - d_0}{d_0} \right| + \left| \frac{d_2 - d_0}{d_0} \right| \right) \times 100\%, \qquad (2)$$

where $d_0$ is the pitch of wave for mold and $d_1$ and $d_2$ are the pitches of two adjacent waves for BMCS. Two specimens were taken from the adjacent wave of each replicated sheet for the deformation ratio test.

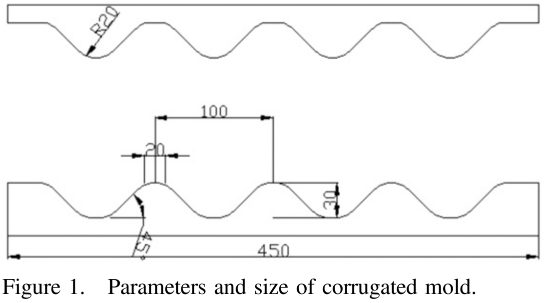


Figure 1. Parameters and size of corrugated mold.

Failing load was determined by loading on the corrugated bridge specimens (100 mm × 20 mm × 6 mm), in accordance with the standard procedures in Chinese standard GB/T 7019-2014. Three specimens were taken from each replicated sheet for the failing load test. Three-point bending tests were performed according to the Chinese standard GB/T 17657-2013, using an Instron 5582 universal testing machine. Six specimens (150 mm [length] × 20 mm [width] × 6 mm [thickness]) were taken from the flat section of each replicated sheet (Fig 2) for the static bending test.

Izod impact tests were performed on unnotched specimens using a CEAST model 6957 impact tester according to the Chinese standard GB/T

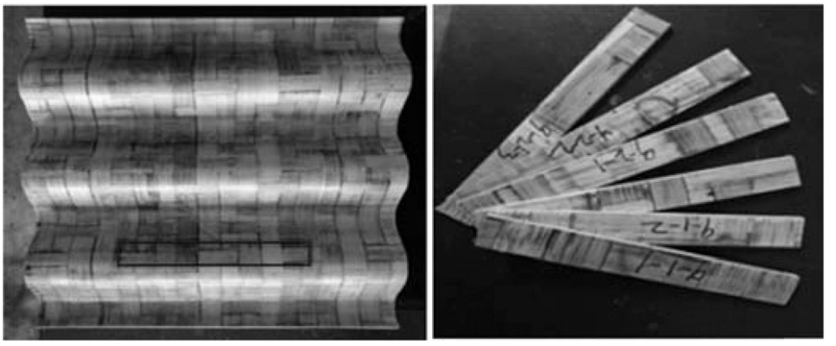

Figure 2. Specimens cut from flat section of bamboo mat corrugated sheet for testing.

1843-2008. Six specimens (80 mm × 10 mm × 6 mm) were taken from the flat section of each replicated sheet for the impact test.

## RESULTS AND DISCUSSION

Our previous study illustrated that keeping MC above 8% would facilitate compression and subsequent fixation of bamboo strips (Gao et al 2018). But too high MC (higher than 15%) can generate a mass of water vapor during pressing, causing bubbles in the panel. Besides, the adhesive would spill over with the water vapor. Therefore, the MC of resinated mat was dried to 9-15% in this study. The pressing time and temperature are also very important because it is necessary to get a high enough temperature in the core to cure the adhesive, and at the same time, the temperature at the surface should not be too high to avoid severe thermal degradation (Monteiro et al 2018). Based on the differential scanning calorimetry curve of PF resin and thermal degradation temperature of bamboo, the levels of pressing temperature and time were selected.

### Regression Models and ANOVA

Experimental results, including deformation ratio, failing load, bending srength, and impact strength are presented in Table 2. To evaluate the statistical significance of the process factors and sufficiency of the model, ANOVA test was applied. Tables 3-6 give the initial ANOVA results for the four properties. Significant quadric models were obtained for all these properties

Table 3. Initial analysis of variance results for response surface quadratic model of deformation ratio.

| Source | Sum of squares | *df* | Mean square | *F* value | *p* value |
|---|---|---|---|---|---|
| Model | 83.80 | 9 | 9.31 | 12.97 | 0.0014 |
| *A*-MC | 63.28 | 1 | 63.28 | 88.16 | <0.0001 |
| *B*-temperature | 0.28 | 1 | 0.28 | 0.39 | 0.5512 |
| *C*-time | 1.80 | 1 | 1.80 | 2.51 | 0.1568 |
| *AB* | 1.69 | 1 | 1.69 | 2.35 | 0.1688 |
| *AC* | 0.12 | 1 | 0.12 | 0.17 | 0.6919 |
| *BC* | 0.42 | 1 | 0.42 | 0.59 | 0.4680 |
| $A^2$ | 9.41 | 1 | 9.41 | 13.11 | 0.0085 |
| $B^2$ | 1.75 | 1 | 1.75 | 2.44 | 0.1622 |
| $C^2$ | 3.56 | 1 | 3.56 | 4.96 | 0.0611 |
| Lack of fit | 1.69 | 3 | 0.56 | 0.68 | 0.6100 |
| Pure error | 3.33 | 4 | 0.83 | — | — |
| Corrected total | 88.82 | 16 | — | — | — |

$R^2 = 0.9434$, adjusted $R^2 = 0.8707$, and predicted $R^2 = 0.6365$.

Table 4. Initial analysis of variance results for response surface quadratic model of failing load.

| Source | Sum of squares | *df* | Mean square | *F* value | *p* value |
|---|---|---|---|---|---|
| Model | 2.514E+005 | 9 | 27,934 | 73.35 | <0.0001 |
| *A*-MC | 33,800 | 1 | 33,800 | 88.75 | <0.0001 |
| *B*-temperature | 8978 | 1 | 8978 | 23.57 | 0.0018 |
| *C*-time | 6962 | 1 | 6962 | 18.28 | 0.0037 |
| *AB* | 17,956 | 1 | 17,956 | 47.15 | 0.0002 |
| *AC* | 3600 | 1 | 3600 | 9.45 | 0.018 |
| *BC* | 19,044 | 1 | 19,044 | 50 | 0.0002 |
| $A^2$ | 42,952 | 1 | 42,951 | 112.78 | <0.0001 |
| $B^2$ | 59,625 | 1 | 59,625 | 156.56 | <0.0001 |
| $C^2$ | 41,685 | 1 | 41,685 | 109.45 | <0.0001 |
| Lack of fit | 218 | 3 | 72.67 | 0.12 | 0.9444 |
| Pure error | 2448 | 4 | 612 | | |
| Corrected total | 2.541E+005 | 16 | | | |

$R^2 = 0.9895$, adjusted $R^2 = 0.9760$, and predicted $R^2 = 0.9712$.

indicated by *p* values less than 0.05. The lack of fit is the variation of the data around the fitted model, which is a special investigative test for adequacy of a model fit. If the model does not fit the data well, the lack of fit will be significant (Yaghoobi and Fereidoon 2018b). In this study, with regard to all the tested properties, the lack of fit is insignificantly relative to the pure error, indicating good fit of the model. In addition to lack of fit tests, the model was further evaluated by the observed vs predicted plot. The points of all predicted and actual responses fell in 45° lines, indicating good response to the model. The normal probability plots also indicated a good agreement between the experimental results and those predicted by the model.

The significance of main and interaction effects in the predictive model was considered based on their *p* values. *p* value less than 0.05 indicates model terms are significant. The insignificant terms were removed from the final expression of the model. For failing load, all the terms (MC, temperature, and time) and the interactions among them were significant model terms, so the model reduction was not performed on it. To improve the model, ANOVA for deformation ratio and bending strength was repeated after eliminating insignificant terms, and the results are shown in Tables 7 and 8. The *p* value of the remaining terms was reduced after omitting insignificant ones. Moreover, the *p* value of "lack of fit" for the responses was increased, indicating the

Table 5. Initial analysis of variance results for response surface quadratic model of bending strength.

| Source | Sum of squares | *df* | Mean square | *F* value | *p* value |
|---|---|---|---|---|---|
| Model | 6750.53 | 9 | 750.06 | 33.53 | <0.0001 |
| *A*-MC | 7.60 | 1 | 7.60 | 0.34 | 0.5781 |
| *B*-temperature | 571.22 | 1 | 571.22 | 25.53 | 0.0015 |
| *C*-time | 1441.84 | 1 | 1441.84 | 64.45 | <0.0001 |
| *AB* | 578.40 | 1 | 578.40 | 25.86 | 0.0014 |
| *AC* | 9.30 | 1 | 9.30 | 0.42 | 0.5396 |
| *BC* | 2.72 | 1 | 2.72 | 0.12 | 0.7375 |
| $A^2$ | 2023.56 | 1 | 2023.56 | 90.46 | <0.0001 |
| $B^2$ | 1108.08 | 1 | 1108.08 | 49.53 | 0.0002 |
| $C^2$ | 603.54 | 1 | 603.54 | 26.98 | 0.0013 |
| Lack of fit | 96.22 | 3 | 32.07 | 2.13 | 0.2398 |
| Pure error | 60.37 | 4 | 15.09 | — | — |
| Corrected total | 6907.12 | 16 | — | — | — |

$R^2 = 0.9773$, adjusted $R^2 = 0.9482$, and predicted $R^2 = 0.7634$.

Table 6. Initial analysis of variance results for response surface quadratic model of impact strength.

| Source | Sum of squares | *df* | Mean square | *F* value | *p* value |
|---|---|---|---|---|---|
| Model | 307.83 | 9 | 34.20 | 44.41 | <0.0001 |
| *A*-MC | 27.42 | 1 | 27.42 | 35.60 | 0.0006 |
| *B*-temperature | 13.03 | 1 | 13.03 | 16.92 | 0.0045 |
| *C*-time | 4.15 | 1 | 4.15 | 5.38 | 0.0534 |
| *AB* | 35.88 | 1 | 35.88 | 46.59 | 0.0002 |
| *AC* | 16.04 | 1 | 16.04 | 20.83 | 0.0026 |
| *BC* | 2.81 | 1 | 2.81 | 3.64 | 0.0980 |
| $A^2$ | 20.55 | 1 | 20.55 | 26.68 | 0.0013 |
| $B^2$ | 42.42 | 1 | 42.42 | 55.08 | 0.0001 |
| $C^2$ | 127.21 | 1 | 127.21 | 165.17 | <0.0001 |
| Lack of fit | 4.22 | 3 | 1.41 | 4.79 | 0.0823 |
| Pure error | 1.17 | 4 | 0.29 | | |
| Corrected total | 313.22 | 16 | | | |

$R^2 = 0.9828$, adjusted $R^2 = 0.9607$, and predicted $R^2 = 0.7788$.

fitness of model was improved. It should be noted that although the interaction effect of BC was insignificant for impact strength, ANOVA indicated that the elimination of BC did not improve the model. Thus, model reduction was not performed on impact strength.

The final predicted models in terms of significant factors for deformation ratio, failing load, bending strength, and impact strength are given as follows:

$$\text{Deformation ratio} = +2.16 - 2.81 * A + 1.58 * A^2, \quad (3)$$

$$\text{Failing load} = +546.00 - 65.00 * A + 33.50 * B + 29.50 * C + 67.00 * A * B + 30.00 * A * C - 69 * B * C - 101.00 * A^2 - 119.00 * B^2 - 99.50 * C^2, \quad (4)$$

$$\text{Bending strength} = +183.82 + 0.98 * A + 8.45 * B + 13.43 * C - 12.03 * A * B - 21.92 * A^2 - 16.22 * B^2 - 11.97 * C^2, \quad (5)$$

$$\text{Impact strength} = +37.00 - 1.86 * A - 1.26 * B - 0.72 * C + 2.97 * A * B - 2.00 * A * C + 0.85 * B * C - 2.21 * A^2 - 3.16 * B^2 - 5.49 * C^2. \quad (6)$$

Here *A*, *B*, and *C*, as shown in Table 1, are MC, pressing temperature, and pressing time, respectively.

## Factors Affecting Deformation Ratio

It is observed from ANOVA for deformation ratio that the linear and quadratic effect of MC significantly influenced deformation ratio (Table 7).

Table 7. Final analysis of variance results for response surface quadratic model of deformation ratio.

| Source | Sum of squares | *df* | Mean square | *F* value | *p* value |
|---|---|---|---|---|---|
| Model | 73.88 | 2 | 36.94 | 34.62 | <0.0001 |
| *A*-MC | 63.28 | 1 | 63.28 | 59.30 | <0.0001 |
| $A^2$ | 10.60 | 1 | 10.60 | 9.93 | 0.0071 |
| Lack of fit | 11.61 | 10 | 1.16 | 1.39 | 0.4011 |
| Pure error | 3.33 | 4 | 0.83 | — | — |
| Corrected total | 88.82 | 16 | — | — | — |

$R^2 = 0.8318$, adjusted $R^2 = 0.8078$, and predicted $R^2 = 0.7755$.

Table 8. Final analysis of variance results for response surface quadratic model of bending strength.

| Source | Sum of squares | *df* | Mean square | *F* value | *p* value |
|---|---|---|---|---|---|
| Model | 6738.50 | 7 | 962.64 | 51.38 | <0.0001 |
| *A*-MC | 7.60 | 1 | 7.60 | 0.41 | 0.5399 |
| *B*-temperature | 571.22 | 1 | 571.22 | 30.49 | 0.0004 |
| *C*-time | 1441.84 | 1 | 1441.84 | 76.96 | <0.0001 |
| *AB* | 578.40 | 1 | 578.40 | 30.87 | 0.0004 |
| $A^2$ | 2023.56 | 1 | 2023.56 | 108.01 | <0.0001 |
| $B^2$ | 1108.08 | 1 | 1108.08 | 59.14 | <0.0001 |
| $C^2$ | 603.54 | 1 | 603.54 | 32.21 | 0.0003 |
| Lack of fit | 108.25 | 5 | 21.65 | 1.43 | 0.3742 |
| Pure error | 60.37 | 4 | 15.09 | — | — |
| Corrected total | 6907.12 | 16 | — | — | — |

$R^2 = 0.9756$, adjusted $R^2 = 0.9566$, and predicted $R^2 = 0.8568$.

Pressing temperature and time were not significant model terms for deformation ratio. As the MC increased while the other two factors remained constant, deformation ratio decreased gradually. This indicated keeping higher MC would facilitate deformation fixation. Our previous study also confirmed keeping MC above 8% would facilitate compression and subsequent fixation for bamboo, attributed to the plasticizing effect of water (Gao et al 2018).

## Factors Affecting Failing Load, Bending Strength, and Impact Strength

With respect to failing load, all single factors (MC, temperature, and time) and the interactions between any two of them were significant model terms (Table 4). Figure 3 exhibits the interaction effect among three factors on failing load. Failing load at high MC (15%), low pressing temperature (130°C), and short pressing time (6 min) was relatively poor. This might be attributed to too low hot-press temperature and short hot-press time as these factors do not fulfill the requirements of a desired curing condition. Increasing the MC initially increased and then decreased the failing load value (Fig 3[a] and [b]). This indicated that the MC higher than a specified value produced a negative effect on the performance. Excessive moisture might lead to blow or blisters on sheets. Failing load was increased with increasing pressing temperature and time but slowly decreased after a certain point (Fig 3[c]). The interaction effect of MC and pressing temperature generate similar trends on failing load with that of MC and pressing time. The highest failing load was obtained when pressed for 12 min at 145°C with 12% MC.

For bending strength, the pressing temperature and time were significant single factors. There was an interaction between MC and temperature, which was a significant model term (Table 8). The interaction influence of MC and pressing temperature on bending strength is shown in Fig 4. The 3D surface graph showed that when the pressing time remained constant at its middle value (12 min), the low MC (9%) and pressing temperature (130°C) resulted in lowest bending strength (127 MPa). The high bending strength depended on the combined effect of moderate MC and high pressing temperature (160°C). High pressing temperature ensures adequate heat in the core and formation of consolidated composites. Heat transfer to the center of a mat in a hot press is strongly influenced by MC. Islam et al (2012) reported that boards produced from particles with 10-18% MC (after adding adhesive) exhibited faster increase in temperature at the beginning of the pressing process because of good conductivity of water and water vapor; thus, heat was transferred from heating press platens to the inside of the board faster and uniformly.

With respect to impact strength, MC and pressing temperature were significant factors, along with the second-order main effects ($A^2$, $B^2$, and $C^2$) and

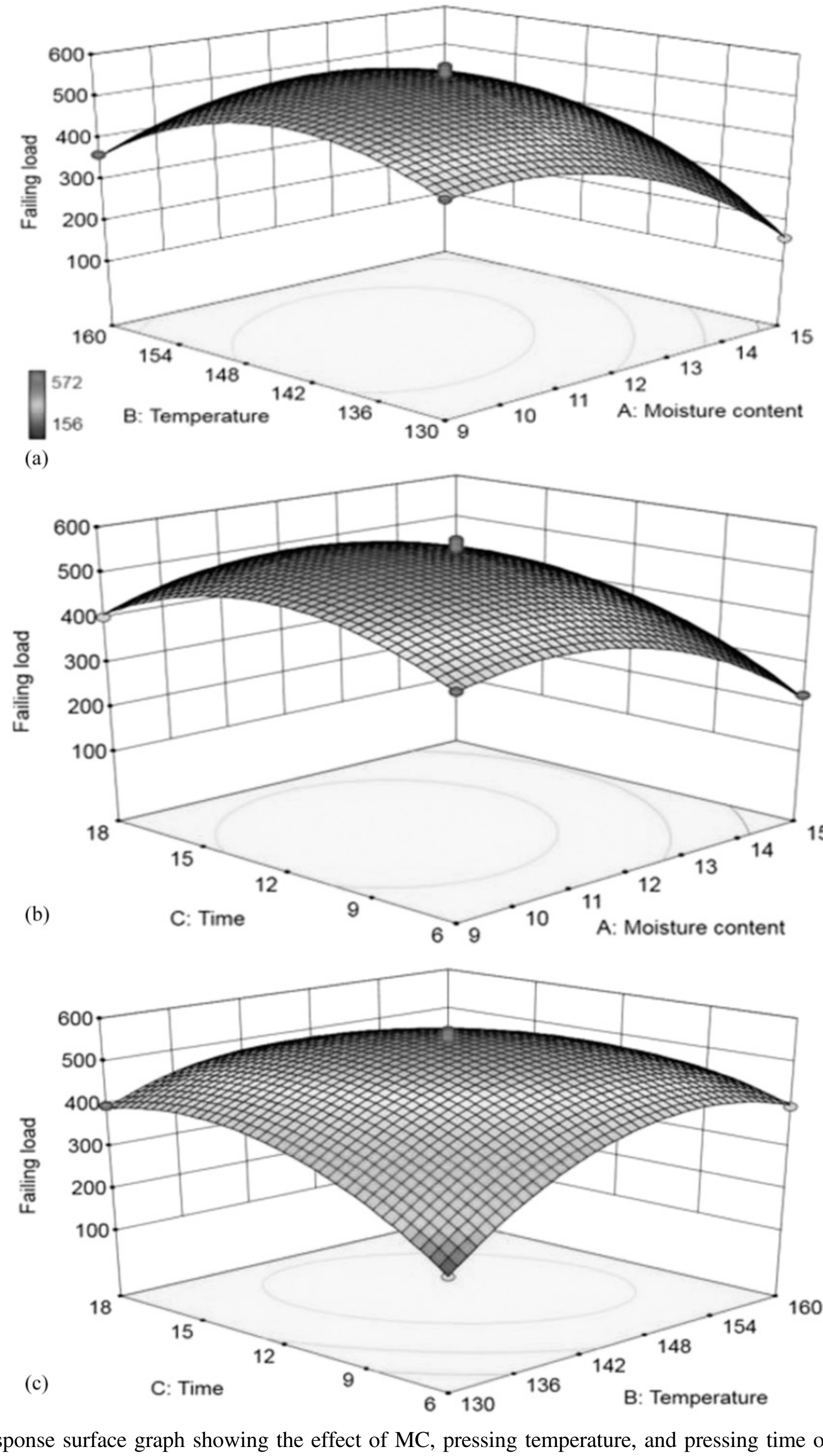


Figure 3. Response surface graph showing the effect of MC, pressing temperature, and pressing time on failing load.

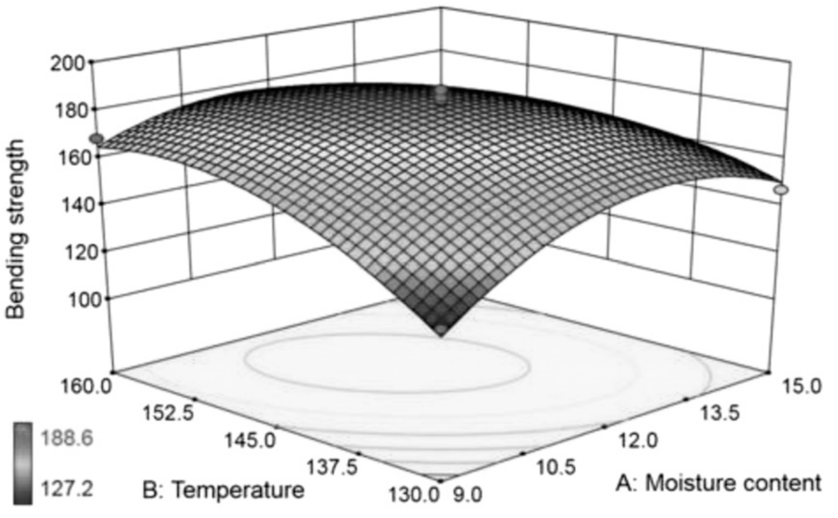


Figure 4. Response surface graph showing the effect of MC and pressing temperature on bending strength.

the *AB* and *AC* interactions (Table 6). The interaction effect of MC, pressing temperature, and pressing time on impact strength is shown in Fig 5. The highest impact strength was obtained with MC, pressing temperature, and time at their middle values. A further increase in pressing temperature and time led to decreased impact strength. The negative impact of higher pressing temperature and longer pressing time on strength properties was possibly due to overcuring of resin and degradation of chemical components of bamboo (Zhao et al 2008). A previous study on thermal treatment on bamboo by Zhang et al (2012) illustrated that the modulus of rupture reduced significantly with increasing temperature and duration when samples were heat-treated above 160°C, which is strongly correlated with the degradation of holocellulose.

## Optimization by Derringer's Desirability Function

The multiresponse optimization process was carried out by using response optimizer part of the Design-Expert software. Four responses (deformation ratio, failing load, bending strength, and impact strength) were simultaneously optimized by Derringer's desirability function. A detailed description of this desirability functions was reported by Islam et al (2010). The optimal solution was found to be MC 12.3%, pressing temperature 146.2°C, and pressing time 12.8 min. Under these conditions, the optimized low value of deformation ratio and high values of mechanical properties were attained simultaneously. The predicted properties were 1.8% for deformation ratio, 542 N for failing load, 185.7 MPa for bending strength, and 36.5 kJ/m$^2$ for impact strength.

To validate the statistical experimental strategies, a confirmation experiment was performed. Samples were prepared by using the optimized variables obtained by the BBD. The experimental values of deformation ratio, failing load, bending strength, and impact strength were 1.7%, 532 N, 188.6 MPa, and 34.6 kJ/m$^2$, respectively. Results demonstrated that the percentage error between the measured and predicted values was well within the value of 6%. Good agreement between the predicted and experimental results verified validity of the model and confirmed existence of the optimal point.

## CONCLUSION

BBD offers a better insight into the interactive effects of three processing variables (MC, pressing temperature, and pressing time) on the properties of BMCS. The prediction based on a quadratic model was in good agreement with the experimental results. Numerical optimization was used

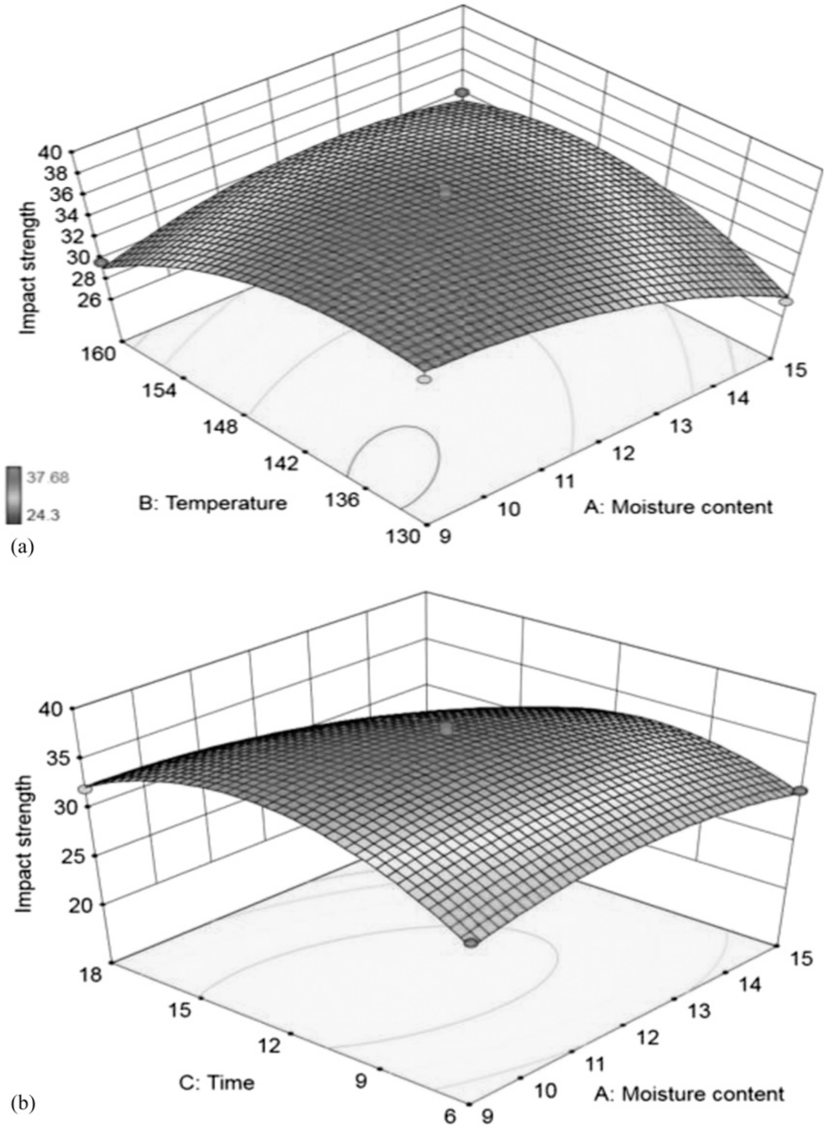


Figure 5. Response surface graph showing the effect of MC, pressing temperature, and pressing time on impact strength.

to determine the conditions for manufacturing the composites with optimized low deformation ratio and high mechanical strength. The optimum parameters were determined as MC 12.3%, pressing temperature 146.2°C, and pressing time 12.8 min. A confirmation study was performed on samples prepared with the optimum process parameters. The results of optimized sample from experimental test were in good agreement with the optimized data by BBD. RSM with desirability functions has been proven to be adequate for the design and optimization of the process parameters for the BMCS production.

**ACKNOWLEDGMENT**

The authors acknowledge the sponsorship from Special Fund of Chinese Academy of Forestry for Fundamental Scientific Research (No. CAFYBB2014MA009).

## REFERENCES


Bansal AK, Zoolagud SS (2002) Bamboo composites: Material of the future. J Bamboo Rattan 1(2):119-130.

Carlborn K, Matuana LM (2006) Modeling and optimization of formaldehyde-free wood composites using a Box-Behnken design. Polym Compos 27(5):497-503.

Chen F, Jiang Z, Wang G, Shi SQ, Liu X (2013a) Bamboo bundle corrugated laminated composites (BCLC). Part I. Three-dimensional stability in response to corrugating effect. J Adhes 89(3):225-238.

Chen N, Lin Q, Zeng Q, Rao J (2013b) Optimization of preparation conditions of soy flour adhesive for plywood by response surface methodology. Ind Crops Prod 51:267-273.

Dayyani I, Shaw AD, Saavedra Flores EI, Friswell MI (2015) The mechanics of composite corrugated structures: A review with applications in morphing aircraft. Compos Struct 133:358-380.

Gao L, Guo W, Luo S (2018) Investigation of changes in compressed moso bamboo (*Phyllostachys pubescens*) after hot-press molding. J Wood Sci 64(5):557-565.

Islam MA, Alam MR, Hannan MO (2012) Multiresponse optimization based on statistical response surface methodology and desirability function for the production of particleboard. Compos Part B Eng 43(3):861-868.

Islam MA, Nikoloutsou Z, Sakkas V, Papatheodorou M, Albanis T (2010) Statistical optimisation by combination of response surface methodology and desirability function for removal of azo dye from aqueous solution. Int J Environ Anal Chem 90(3-6):497-509.

Jiang Z, Chen F, Wang G, Liu XE, Shi SQ, Yu Z, Cheng HT (2013) Bamboo bundle corrugated laminated composites (BCLC). Part II. Damage analysis under low velocity impact loading. BioResources 8(1):923-932.

Kumar A, Sharma KV, Gupta A, Tywoniak J, Hajek P (2016) Optimization of processing parameters of medium density fiberboard using response surface methodology for multiwalled carbon nanotubes as a nanofiller. Eur J Wood Wood Prod 75(2):203-213.

Monteiro S, Martins J, Magalhães FD, Carvalho L (2018) Lightweight wood composites: Challenges, production and performance. Pages 293-322 *in* S Kalia, ed. Lignocellulosic Composite Materials. Springer, Cham, Switzerland.

Nakhaei MR, Mostafapour A, Naderi G (2017) Optimization of mechanical properties of PP/EPDM/clay nanocomposite fabricated by friction stir processing with response surface methodology and neural networks. Polym Compos 38:E421-E432.

Park KJ, Jung K, Kim YW (2016) Evaluation of homogenized effective properties for corrugated composite panels. Compos Struct 140:644-654.

Toupe JL, Trokourey A, Rodrigue D (2014) Simultaneous optimization of the mechanical properties of postconsumer natural fiber/plastic composites: Phase compatibilization and quality/cost ratio. Polym Compos 35(4):730-746.

Yaghoobi H, Fereidoon A (2018a) An experimental investigation and optimization on the impact strength of kenaf fiber biocomposite: Application of response surface methodology. Polym Bull 75(8):3283-3309.

Yaghoobi H, Fereidoon A (2018b) Modeling and optimization of tensile strength and modulus of polypropylene/kenaf fiber biocomposites using Box-Behnken response surface method. Polym Compos 39:E463-E479.

Yaghoobi H, Fereidoon A (2018c) Thermal analysis, statistical predicting, and optimization of the flexural properties of natural fiber biocomposites using Box–Behnken experimental design. J Nat Fibers, 1-19.

Yang F, Fei B, Wu Z, Peng L, Yu Y (2014) Selected properties of corrugated particleboards made from bamboo waste (*Phyllostachys edulis*) laminated with medium-density fiberboard panels. BioResources 9(1):1085-1096.

Yu YS, Ni CY, Yu T, Wan H (2015) Optimization of mechanical properties of bamboo plywood. Wood Fiber Sci 47(1):109-119.

Zhang YM, Yu YL, Yu WJ (2012) Effect of thermal treatment on the physical and mechanical properties of *Phyllostachys pubescens* bamboo. Eur J Wood Wood Prod 71(1):61-67.

Zhao J, Wang XM, Chang JM, Zheng K (2008) Optimization of processing variables in wood-rubber composite panel manufacturing technology. Biores Technol 99(7):2384-2391.